Biochimica et Biophysica Acta 1837 (2014) 418–426

Contents lists available at ScienceDirect

Biochimica et Biophysica Acta

journal homepage: www.elsevier.com/locate/bbabio

Review

Structures of mitochondrial oxidative phosphorylation supercomplexes and mechanisms for their stabilisation ☆

Yuriy Chaban [a,1], Egbert J. Boekema [b], Natalya V. Dudkina [b,*,2]

[a] Institute of Structural and Molecular Biology, Malet street, Birkbeck College, London WC1E 7HX, UK
[b] Electron Microscopy Group, Groningen Biomolecular Sciences and Biotechnology Institute, University of Groningen, Nijenborgh 7, 9747AG Groningen, The Netherlands

ARTICLE INFO

Article history:
Received 28 July 2013
Received in revised form 1 October 2013
Accepted 15 October 2013
Available online 30 October 2013

Keywords:
Oxidative phosphorylation
Mitochondria
Supercomplex
ATP synthase
Electron microscopy

ABSTRACT

Oxidative phosphorylation (OXPHOS) is the main source of energy in eukaryotic cells. This process is performed by means of electron flow between four enzymes, of which three are proton pumps, in the inner mitochondrial membrane. The energy accumulated in the proton gradient over the inner membrane is utilized for ATP synthesis by a fifth OXPHOS complex, ATP synthase. Four of the OXPHOS protein complexes associate into stable entities called respiratory supercomplexes. This review summarises the current view on the arrangement of the electron transport chain in mitochondrial cristae. The functional role of the supramolecular organisation of the OXPHOS system and the factors that stabilise such organisation are highlighted. This article is part of a Special Issue entitled: Dynamic and ultrastructure of bioenergetic membranes and their components.

1. Introduction

Mitochondria play a number of vital roles in the eukaryotic cell, among which the most important one is the production of ATP during oxidative phosphorylation (OXPHOS). The heavily folded inner membranes of mitochondria called cristae accommodate many copies of the respiratory chain components, or OXPHOS complexes (I–IV). Together with ATP synthase (complex V) they form the machinery for production of ATP, the energy currency of the cell. Complexes I–IV are multisubunit enzymes that work in concert to create an electrochemical proton gradient across the mitochondrial inner membrane that is used by the F_1F_o ATP synthase (complex V) to produce ATP via oxidative phosphorylation, although complex II is not directly able to pump protons. NADH or succinate, generated during glycolysis, fatty acid oxidation and in the citric acid cycle, form the fuel for the respiratory chain. During catalysis, there is electron transfer between the complexes mediated by two small components: lipid-soluble ubiquinone and water-soluble cytochrome *c*. They diffuse between the respiratory complexes I and III, and III and IV, respectively, and the latter takes them to form water from molecular oxygen (Fig. 1).

For understanding OXPHOS at the molecular level it was all-important that atomic structures of the individual complexes were solved. *Complex I* or NADH dehydrogenase is the largest enzyme of the electron transport chain (ETC) and has a characteristic L shape with an extensive part being embedded in the lipid bilayer and a smaller shoulder protruding into the mitochondrial matrix. The recent X-ray structure of the bacterial complex I suggests the coupling mechanism for NADH dehydrogenase [1]. Complex I binds NADH substrate to the distal end of the hydrophilic arm and transfers two electrons, one at a time, via FMN and seven iron–sulphur clusters to the bound ubiquinone at the interface between two arms [2]. Reduction of the ubiquinone induces conformational changes in the membrane arm resulting in translocation of four protons across the membrane via four channels [1].

Complex II or succinate dehydrogenase is the second independent entrance point of electrons to the respiratory chain. It oxidises succinate and transfers electrons through three iron–sulphur clusters to ubiquinone. Complex II is not a proton pump and it does not contribute directly to the proton gradient formation.

Complex III or cytochrome *c* oxidoreductase, which is known to exist in the membrane as a dimer, oxidises ubiquinone to ubiquinol and as a result it can pump two protons to the intermembrane space. The electrons from ubiquinol are passed to the carrier cytochrome *c* via cytochromes *b* and c_1 of complex III.

The last enzyme of the mitochondrial electron transport chain is *complex IV* or cytochrome *c* oxidase. It accepts electrons from cytochrome *c* and delivers them to an oxygen molecule to convert it to two water molecules. Four protons are pumped to the intermembrane space during this process.

☆ This article is part of a Special Issue entitled: Dynamic and ultrastructure of bioenergetic membranes and their components.

* Corresponding author at: Institute of Structural and Molecular Biology, Birkbeck College, Malet street, London WC1E 7HX, UK.
E-mail address: n.dudkina@mail.cryst.bbk.ac.uk (N.V. Dudkina).
[1] Current address: Division of Structural Biology, Chester Beatty Laboratories, The Institute of Cancer Research, 237 Fulham Road, London SW3 6JB, United Kingdom
[2] Current address: Institute of Structural and Molecular Biology, Birkbeck College, Malet street, London WC1E 7HX, UK.

0005-2728/$ – see front matter © 2013 Elsevier B.V. All rights reserved.
http://dx.doi.org/10.1016/j.bbabio.2013.10.004

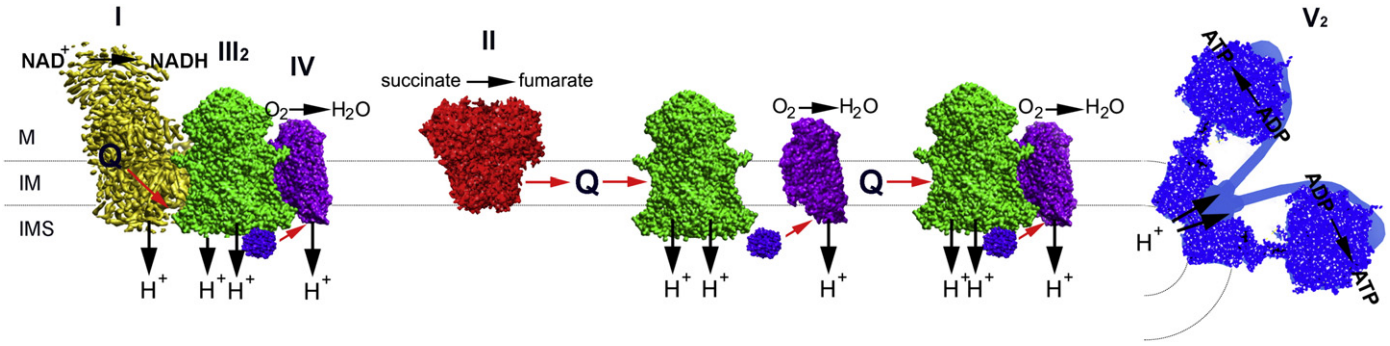

Fig. 1. Plasticity model of the mitochondrial electron transport chain in which complexes I–IV are partly organised into supercomplexes, except for complex II, which feeds electrons via ubiquinone to complex III non-bound to complex I. Red arrows show electron pathways. In yellow, the complex I, marked as I; in red the complex II, marked as II; in green the complex III_2, marked as III_2; in purple the complex IV, marked as IV; in blue the dimeric ATP synthase, marked as V_2; in violet the cytochrome *c*; Q, ubiquinol. The positions of the matrix (M), the intermembrane space (IMS) and cristae or inner membrane (IM) are indicated.

ATP synthase or complex V uses the energy stored in a proton gradient to turn ADP into ATP. It is a complex formed by 15–18 subunits with a total mass of 600 kDa [3]. The water-soluble F_1-part consists of three α and three β catalytic subunits. The F_1-part is connected to the membrane-embedded ring-like subunit c oligomer of the F_o-part by a central and a peripheral stalk. The F_o-part is composed of subunits a (Su 6), A6L (Su 8), e, f, g, the central stalk consists of the γ, δ and ε subunits and the peripheral stalk is made from subunits OSCP (Su 5), b, d, F6 (h) (the nomenclature of subunits in yeast is indicated in brackets, reviewed in [4]). The yeast enzyme has two specific additional subunits, i and k, which belong to the membrane part. Protons cross the membrane via the proton channel in the membrane part rotating the multi-subunit c ring and the central stalk. The αβ trimer of F_1-part is prevented from rotation by the peripheral stalk and catalyses ATP synthesis via the binding change mechanism [5].

2. Supramolecular organisation of the respiratory chain

The most important experimental strategy to characterise the organisation of the OXPHOS system has been blue-native polyacrylamide gel electrophoresis (BN-PAGE), first introduced by Hermann Schägger and colleagues [6,7]. BN-PAGE is based on the mild solubilisation of mitochondrial membranes with non-ionic detergents and is able to separate the largest stable protein complexes that can withstand solubilisation. This technique allowed the separation of respiratory supercomplexes on gels and marked the beginning of the study of the higher level of structural organisation of the OXPHOS system. Electron microscopy single particle analysis provided the first structural evidence for the respiratory supercomplexes [8,9]. In the last two decades, BN-PAGE and other biochemical techniques have triggered a considerable change in the view on the organisation of the electron transport chain in mitochondrial membranes. The idea of random diffusion of complexes in cristae was ruled out by a number of experiments. Flux-control measurements combined with inhibitor titration revealed that the yeast electron transport chain behaves as a single functional unit [10,11].

Respiratory supercomplexes have been found in organisms belonging to different kingdoms of eukaryotes (Table 1). Despite their phylogenetic distances from each other, all of them have in common that their OXPHOS systems have supramolecular organisation. Based on composition, all supercomplexes can be divided into four main groups. Complexes I, III_2 and IV were found to assemble into I + III_2, III_2 + IV_{1-2} or I + III_2 + IV_{1-4} supercomplexes. ATP synthases form dimers, which constitute oligomeric chains in cristae. Complex II is the only enzyme of the respiratory chain, which does not associate with the other respiratory complexes. Although Acin-Perez et al. reported complex II to be a part of the mouse respirasome, which is able to transfer electrons from succinate [12], this was not supported by any other studies. Unlike the other enzymes of the OXPHOS system, complex II is not only involved into respiration but also directly participates in the citric acid cycle. This could explain why complex II was not found to be part of the respiratory supercomplexes. Interestingly, a recent study revealed that the electron flow from the FAD substrate to complex III is independent from the electron pathway that originates from NAD^+ and takes place within the I + III_2 supercomplex ([13] Fig. 1). These two pathways use two different populations of quinone [13]. The abundance of the supercomplexes with different compositions varies from the organism to the organism. Thus, the supercomplex with composition I + III_2 is the most abundant in plants ([14], Table 1), where 90–100% of complex IV is found in the monomeric form [15]. I + III_2 + IV_{1-4} supercomplex is higher in abundance in mammals [7] and III_2 + IV_2 in fungi [7,16].

Structural studies of mitochondrial membranes revealed supramolecular assemblies of the OXPHOS system in situ. Rapid-freeze deep-etch electron microscopy provided the first demonstration of oligomeric rows of ATP synthase dimers in mitochondria of *Paramecium* in 1989 [17]. This work also suggested ordered linear arrays of the complex I in cristae [17]. The emergence of cryo-electron tomography (ET) has given rise to the study of supramolecular organisation of the respiratory

Table 1
[a]Representation of respiratory supercomplexes in the various kingdoms of living organisms.

Organism		I+III_2	III_2+IV_{1-2}	I+III_2+IV_{1-4}	V_2	Refs
Plants	*Arabidopsis thaliana*	x			x	[14]
	Hordeum vulgare	x				[14]
	Phaseolus vulgaris	x				[14]
	Solanum tuberosum	x[b]	x	x	x	[14,15,28]
	Spinacia oleracea	x	x	x	x	[29]
	Nicotiana sylvestris	x				[87]
	Pisum sativum	x				[88]
	Helianthus annuus			(x)[c]		[89]
	Zea mays	x			x	[27,66]
	Asparagus officinalis	x	x			[30]
Algae	*Chlamydomonas reinhardtii*				x	[90]
	Polytomella sp.	x			x	[8,91]
Fungi	*S. cerevisiae*	-[d]	x	-[d]	x	[6,7]
	Yarrowia lipolytica	x[e]	x	x[e]	x	[20,92]
	Podospora anserina	x	x	x	x	[93,96]
	Neurospora crassa		x	x[e]	x	[97]
Protozoa	*Tetrahymena thermophila*	x			x	[63]
	Plasmodium falciparum				x	[94]
Animals	*Bos taurus*	x	x	x	x	[7]
	Homo sapiens	x	x	x	x	[95,98]

[a] Empty cells in the table indicate that the corresponding supercomplexes have not been discovered.
[b] In potato, two forms of I + III supercomplexes occur, which have I + III_2 and I_2 + III_4 composition.
[c] In sunflower, a complex IV containing supercomplex of >1000 kDa was described, which probably has I + III_2 + IV_{1-4} composition.
[d] The OXPHOS system of *S. cerevisiae* does not have complex I and, therefore, contains no I + III_2 and I + III_2 + IV_{1-4} supercomplexes.
[e] In *Neurospora crassa* and *Yarrowia lipolytica*, a I_2 supercomplex was described.

chain in cristae membranes and intact mitochondria without using any fixatives at a resolution that allows the visualisation of individual macromolecules. A number of cryo-ET studies have demonstrated the existence of oligomeric chains of ATP synthases in the cristae membranes of various organisms [18–21]. Results of these experiments suggest different arrangements of the respiratory enzymes in tubular and lamellar types of mitochondria. Oligomeric rows of ATP synthases were found along cristae edges of lamellae, while complexes I–IV would be expected on flat surface of the cristae [20]. In contrast, the tubular cristae of the green alga *Polytomella* were fully covered by oligomeric rows of ATP synthases [19], suggesting that the other OXPHOS enzymes might be arranged in between, but these could not be visualised due to the tight packing of ATP synthases. Interestingly, in tomographic reconstructions of mitochondria from some organisms as bovine, yeast, *Arabidopsis* etc. it is very hard to observe oligomeric chains of dimeric ATP synthases ([20], Dudkina unpublished data), but *Polytomella* is an exception to the rule [19]. A possible explanation is that the dense matrix of the organelles in most organisms obscures many of the internal features [20]. Another explanation could be the variable abundance of ATP synthase complexes among various organisms. Alternatively, ATP synthases could undergo rearrangement in membranes as the dimeric ATP synthases do not physically interact with each other and may drive the deformation of cristae membranes as suggested recently [21].

3. Significance of the OXPHOS supercomplexes

The structural study of the OXPHOS supercomplexes is of special importance for understanding the function of the respiratory chain complexes. Most mitochondrial diseases and disorders, including Parkinson's and Alzheimer's diseases [22,23], are associated with genes that encode for OXPHOS proteins. In addition, mitochondrial dysfunction appears to be a factor in cancer etiology. Mutations of the mitochondrial or nuclear DNA that affect components of the mitochondrial OXPHOS system result in reactive oxygen species (ROS) overproduction and promote tumour cell proliferation [24]. Furthermore, modifications in the levels of ROS have been linked to the resistance of cancer stem cells to chemotherapy [25]. Therefore, the OXPHOS system appears to be an attractive drug target in treatment of cancer and mitochondria-associated diseases. Understanding the supramolecular organisation of the OXPHOS system and its role in functioning of the respiratory chain is essential for the development of such treatment.

4. Respiratory supercomplexes

Complexes I, III_2 and IV form three types of supercomplexes. One copy of complex I can associate with a dimeric complex III to form the I + III_2 supercomplex, which is mainly found in plant mitochondria (Table 1). Electron microscopy revealed that the complex III_2 is laterally attached to the membrane arm of complex I in its concave portion [26–28]. In some organisms complex III_2 was found to associate with one or two copies of complex IV [16,28–30]. The III_2 + $IV_{1–2}$ supercomplex is the most stable in *Saccharomyces cerevisiae*, which lacks complex I. No free monomeric or dimeric forms of complex IV could be detected upon detergent solubilisation [16], indicating that all complex IV makes part of the supercomplex. The detailed EM analysis revealed that the complex III_2 is flanked from both sides by monomeric complexes IV [16]. This study established that complex IV is not a functional dimer as previously proposed on the basis of crystallization experiments [31]. A pseudo-atomic 3D model showed that the monomeric cytochrome *c* oxidase complexes are attached to dimeric complex III at two alternate sides with their convex sides facing the complex III_2 [16]. This is opposite to the side involved in the formation of complex IV dimers as described by X-ray crystallography. The recent cryo-EM map of the supercomplex is in agreement with the pseudo-atomic model, which was based on the negatively stained projections [32]. From the cryo data authors concluded that the distance between cytochrome *c* binding sites in complexes III and IV is about 6 nm [32], in contrast to the shorter 4 nm predicted from the 2D averages [16].

The largest respiratory chain supercomplex is formed by complexes I, III_2 and up to 4 copies of complex IV [7]. It was called the respirasome because it creates the bulk of the proton motive force in the presence of cytochrome *c* and quinone in one unit. Recently, the structure of the bovine respirasome was determined by two different EM methods: cryo-ET of digitonin-solubilised respirasomes [33] and cryo-EM of amphipol-solubilised respirasomes [34]. Both methods gave compatible structures and demonstrated that the complex III_2 sits in the arc of the membrane arm of complex I while complex IV is attached to the tip of NADH dehydrogenase. Docking of X-ray structures of complexes III_2 and IV showed that the interaction sites of complexes III_2 and IV differ from *S. cerevisiae* [31], but in both the yeast and bovine models, the complex IV dimerization interface is free. The differences between the organisation of the bovine and yeast respirasomes might be partly explained by necessity of complex III to interact with both complexes I and IV in mammalian mitochondria. However, even taking into account the interaction between complexes I and III_2 in bovine there is no spatial restriction within the bovine respirasome for the complexes III_2 and IV to interact in the same way as in *S. cerevisiae*. Another possible explanation would be a string-like association between I + III_2 + IV supercomplexes via complexes IV, hypothesized from the respiratory chain fragments resolved on blue-native gels [35]. Early work on *Paramecium* hints to the possible supramolecular organisation of the complex I [17]. However, in the recent work based on cryo-ET authors exclude the existence of such strings [20].

4.1. Stabilising factors for the respirasome

In various organisms respirasomes appear to be very stable because they can be isolated as whole entities without significant degradation. In the last years a lot of effort has been placed into the search for factors that are responsible for gluing together the respirasome components. Cardiolipin is an anionic phospholipid formed by two phosphatidyl groups bound by a glycerol. It is exclusively found in the mitochondrial inner membrane where one of its major roles is to specifically interact with proteins and modulate their functions (reviewed in [36]). The cryo-EM maps of the yeast and bovine respirasomes clearly showed that the complexes I, III_2 and IV are at some distance within the supercomplex in the lipid bilayer and the spaces between complexes appear as a lower density material in the electron microscopy maps [32–34]. Thus, the space is most likely to be filled with lipids. It was shown previously that cardiolipin is required for stability of single complexes III and IV and formation of the stable III_2 + IV_2 supercomplex [37,38]. A content of about 50 molecules of cardiolipins per yeast supercomplex was determined by mass spectrometry analysis [32]. Due to larger distances between complexes, the bovine respirasome can potentially accommodate several times more cardiolipin molecules [34].

Sometimes lipids co-crystallize with membrane protein complexes. In the crystal structure of the bovine complex IV, one cardiolipin molecule was identified at subunit III [39], which is at the interface with complex III in the bovine respirasome EM structure [33], but not in the yeast respirasome [32]. However, photolabeling experiments suggested that the cardiolipin molecule was bound between subunits VIIa and VIIc [40], which are to some extent interacting with complex III in the yeast respirasome [16,32]. Several lipid molecules were found to be associated with the yeast complex III_2. Cardiolipin is bound in a hydrophobic cleft at the interface between cytochromes *b* and c_1 [41]. Cyt *b* and c_1 are facing complex IV in the yeast supercomplex [16], but not in the bovine respirasome. However, a molecular dynamics simulation identified three additional binding sites for cardiolipins, which might be involved in interaction [42]. The authors suggested that the complexes first form an encounter supercomplex by interacting via cardiolipin binding sites. Following this, slow and small rearrangements in the relative orientations of the proteins may occur together with the release of the

excess of cardiolipins from the binding sites. By mass spectrometry it was found that eight and two molecules of cardiolipins associate with complexes III and IV, respectively [43].

Besides lipids, subunit VIIa of cytochrome *c* oxidase and proteins unrelated to the respiratory chain were shown to play a role in the stability of the respirasome. The cytochrome *c* oxidase subunit VIIa polypeptide 2-like (Cox7-a2l) was identified in the respirasome and $III_2 + IV$ supercomplex in mouse fibroblasts, but not in free complexes III or IV [13]. In the absence of Cox7-a2l, complex IV does not assemble into supercomplexes though the electron flux from substrates is not affected. The electrons will pass through a single pool of cyt *c* to a single pool of complex IV [13]. The cytochrome *c* oxidase subunit 7a-related protein (COX7RP) was also identified as a factor that promotes supercomplex assembly [44].

The abundant isoform of the ADP/ATP carrier Aac2, which is facilitating the exchange of ADP and ATP across the mitochondrial inner membrane, was found in association with the $III_2 + IV_{1-2}$ supercomplex [45,46] and it was shown that it requires cardiolipin for proper functioning [45]. Two novel small proteins Rcf1 (respiratory supercomplex factor 1) and Rcf2 (respiratory supercomplex factor 2) of 18 and 25 kDa separately associate with the respirasome and were demonstrated to be important for the stability of the yeast respirasome [47,48]. Rcf1 interacts with the Cox3 subunit of complex IV and is required for the proper assembly and functioning of the supercomplex [47,49]. Rcf1 was found to be in a close proximity to Aac2 [47]. Rcf2 can be specifically found in yeast, while Rcf1 has human homologs RCF1a and RCF1b [48]. Both proteins are found in association with complex IV and Rcf1 plays a crucial role in the stability of the supercomplex. High-resolution structures of the respirasomes will help to assign the positions of these novel components in the supercomplex.

A recent study of the relationship between respiration in mitochondria and cristae ultrastructure suggests that the cristae morphology plays a stabilising role for the respiratory supercomplexes in mice [50].

4.2. Respirasome functions

In the respiratory chain all enzymes are linked by the electron exchange. Ubiquinone physiologically interconnects complexes I and III by accepting electrons from the first and delivering them to the latter. It is known that most of the harmful mitochondrial superoxide originates from complexes I and III [51]. Complexes I and III are assembled within the respirasome such that the ubiquinone binding sites in the bovine respirasome are at a close distance of 13 nm [33,34]. Short movements of ubiquinone make sense not only to speed up the electron transfer process as a whole, but also to minimize loss of the electrons during transfer and the production of harmful oxygen radicals. Another crucial point in the OXPHOS electron pathway is the shuttling of cytochrome *c* between complexes III and IV. Recent data suggest that the distance that cytochrome *c* has to diffuse between the sites of complexes III and IV is 10 nm in the bovine respirasome [33,34], but less than 6 nm in the $III_2 + IV_2$ supercomplex in yeast [32]. Thus, the formation of the respirasome brings these sites closer to each other and is intended to make the transfer more efficient than if complexes III and IV were randomly distributed in the membrane. However, it is questionable if the distance between electron transport components is the main reason for the supercomplex formation. Taking into account that the diameter of cytochrome *c* is about 3.4 nm, Althoff et al. [34] raised the possibility of direct electron channelling of cytochrome *c* between complexes III and IV. However, a strong argument against this conclusion is that the cytochrome *c* binding sites of complexes III and IV are not as close to each other as they could be. Flux control experiments do not provide evidence for substrate channelling between complexes III and IV via cytochrome *c* [11], and a time-resolution spectrophotometric technique has shown that cytochrome *c* is not restricted in its diffusion [52]. Both data rather support the idea that the substrate channelling is not the main reason for the respirasome formation, although substrate channelling was found between bovine complexes I and III via ubiquinone [11].

A recent study of electron flux in the OXPHOS system points to separate pathways in the ETC depending on the presence of the assembly factor Cox7A2l. The complex IV can receive electrons from either the NADH substrate via the $I + III_2/I + III_2 + IV$ supercomplex, from FAD via the complex II and the single complexes III_2 and $IV/III_2 + IV$ supercomplex, or from both NADH and FAD ([13] Fig. 1). Such organisation of the respiratory chain may be essential for optimizing the simultaneous oxidation of multiple substrates [13]. Indeed, the ratio between electrons coming from NADH and FAD is higher when glucose is the main respiratory substrate and lower if fatty-acid oxidation is the main source of substrates [13]. Therefore, the dynamic supramolecular organisation of the ETC might be essential for efficient oxidation of available substrates.

Another intriguing question is how the presence of significant amounts of lipids between single complexes is consistent with the overall efficiency of the electron transfer. Are the lipids ultimately required for the stability of the supercomplex or is their presence a prerequisite for the ubiquinone exchange? Based on the finding that the electron flow from FAD to complex III is independent from the pathway that uses electrons from NAD^+ within the $I + III_2/I + III_2 + IV$ supercomplex [13], we propose that the limited space for lipids between complexes I and III could serve as a diffusion microdomain for the ubiquinone, confining it to the $I + III_2/I + III_2 + IV$ supercomplex. A similar mechanism was suggested for the plastoquinone in chloroplasts [53].

Among other possible functions, the supercomplex can play a role in assembly of its components. Mutations in subunits of complex III or IV destabilize complex I in human and mouse cells [54,55] and complex I is necessary for the full assembly of the complex III in human cells [56,57]. Intriguingly, in the cytoplasmic membrane of the possible ancestor of eukaryotic mitochondria, *Paracoccus denitrificans*, the assembly of respiratory complexes I, III, and IV into the respirasome $I + III_4 + IV_4$ stabilizes the complex I [58].

Finally, the dynamic nature of the respiratory chain has to be taken into account. The supercomplexes can undergo rearrangement in response to the demand for ATP of particular cell types at a given time [59].

5. Dimeric ATP synthase

The first biochemical evidence for a dimeric organisation of the ATP synthase complex in yeast came from the BN-PAGE work by Arnold and colleagues [6]. Later dimers were found in bovine, *Arabidopsis* and several other organisms [7,14]. Interestingly, dimerisation of ATP synthases seems to be a characteristic feature of mitochondria, because no evidence has yet been obtained that supports the existence of dimers in bacterial membranes [60,61]. Structural information about the dimeric ATP synthases comes from either single particle EM of detergent-solubilised proteins or subtomogram averaging in situ. The latter method provides direct insight into supramolecular organisation of macromolecules in membranes but at lower resolution than single particle reconstructions. Low-resolution structures of dimeric ATP synthase were obtained from a wide range of eukaryotes, including the animal *Bos taurus* [9], the alga *Polytomella* sp. [8], the fungus *S. cerevisiae* [21,62], the protozoon *Tetrahymena thermophila* [63] and other organisms (Table 2). Remarkably, these organisms are phylogenetically very distant from each other but nonetheless share similar ultrastructures of the dimeric ATP synthase in their mitochondria (Fig. 2). In nearly all organisms two monomers associate via the membrane F_o parts. A special feature of the dimers is the unusual angle of 40–90° between the monomers, as observed in 2D projections where the dimers are seen from the side (Table 2, Fig. 2a, b, d). However, no such kink between monomers is visible in the EM map of the ATP synthase dimer from *Tetrahymena* (Table 2, Fig. 2c, e).

Table 2
[a]Variation of angles between monomers in dimeric ATP synthases revealed by single particle electron microscopy and electron tomography. Note: the angles are all running inside the plane shown.

Organism	Angles (degrees) by subtomogram averaging *in situ*		Angles by single particle analysis of isolated supercomplexes	
Solanum tuberosum	115	[20]	40	[28]
Polytomella sp.	70	[19]	50	[67]
			70	[8]
Bos taurus	55-90	[18]	40	[9,66]
	80	[20]	90	[66]
Rattus norvegicus	70	[18]	-	
Tetrahymena thermophila	-		0	[this work]
S. cerevisiae	86	[21]	35, 90	[62, 66]
			40	[65]
			55-142	[64]
Yarrowia lipolytica	80	[20]	-	
Podospora anserina	80	[20]	-	

[a] Dashes in the table cells indicate that for the corresponding organism no structural information by the corresponding EM or ET method is available.

5.1. Angular distribution in dimers of ATP synthases

In ATP synthase dimers from different species the interacting monomers make a range of different angles that needs to be discussed. Obviously, detergent treatment during isolation may affect the angle. Several groups observed different angles between monomeric ATP synthases in *S. cerevisiae* using different amounts of detergent. 2D averaging of the dimers extracted with digitonin at a ratio of 5 g per g of protein revealed mainly two types of supercomplexes with angles of either 35° or 90° [62]. A similar study showed that the angles ranged from 55 to 142° for dimers extracted with a digitonin–protein ratio of 1.75 (w/v) [64]. However, in the latter work more than 50% of isolated dimers had angles of 83° or 93°. A third group extracted dimeric ATP synthases in presence of ADP with 2 g of digitonin per g of protein and reported typical angles of 36–48° for their preparation, although they could also find a small number of 90° and 140° dimers [65]. The recent subtomogram averages of the dimeric ATP synthases in yeast in situ did not reveal supercomplexes with small angles and reported only wide-angle dimers of 86° in membranes [21]. This value is more trustworthy because no detergent was used at all and the dimers were observed in their natural environment.

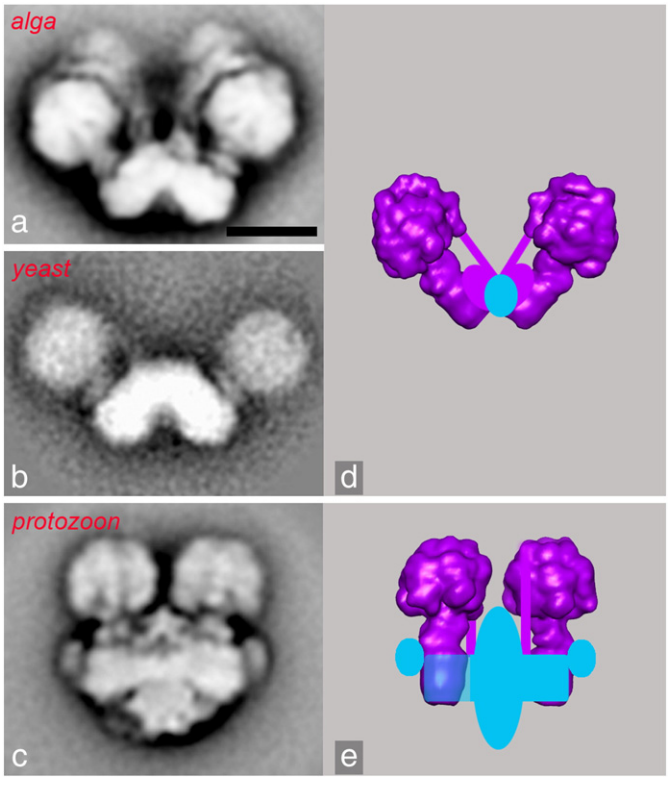

Fig. 2. Dimeric ATP synthases have similar structures in different organisms as revealed by electron microscopy. a–c — 2D averages of dimeric ATP synthases from green alga *Polytomella*, *S. cerevisiae* and protozoon *Tetrahymena*. d — the averaged model of the mitochondrial ATP synthase dimer. e — the model of the dimeric ATP synthase from *Tetrahymena*. The models were generated using atomic coordinates of the yeast F_1c_{10} ATP synthase complex (PDB ID: 2XOK, [81]) and the bovine F_1 and stator subcomplex (PDB ID: 2WSS, [82]). The scale bar is 10 nm.

For the bovine supercomplex, the dimers with an angle of 40° were extracted with the low amount of digitonin 2.5 g per g of protein [9] and a small amount of 90° dimers were found at a ratio 25 g/g [66]. The first reported subtomogram averages of dimeric enzymes in bovine cristae fragments revealed a range of angles between 55 and 95° [18] and the same group later demonstrated that only the angle of 80° is found in membrane fragments [20]. Lower concentrations of detergent seem to increase the level of flexibility between monomers. However, a closer look at the EM averages suggests that the angular difference is likely not only due to flexibility between monomers [62,64,65]. The dimer-specific subunits may also play a role. The wide-angle dimer does not show the same interaction of two monomers as the small-angle dimer because the number of additional subunits located between two F_o-parts is different. The membrane part of the wide-angle dimer is significantly larger than of the narrow-angle dimer and likely has a different composition. Therefore, the previously proposed different breakdown products of the oligomeric chain can still explain the angle difference [62]. The variability of angles between dimers in a row discovered by cryo-ET [21] could explain the variability in the dimer if it is formed by monomers of two neighbouring dimers. In some way, the tomography data must provide a more reliable estimate of angles because tomography can be applied without detergent solubilisation.

In contrast, the dimeric ATP synthase from *Polytomella* seems to be very rigid because both the subtomogram averages and the 2D averages of isolated supercomplexes demonstrated just one fixed angle of 70° [8,19]. A smaller angle of 50° between monomers was reported in a single particle 3D EM study of negatively stained *Polytomella* ATP synthase [67]. However, to establish whether the angle between monomers of ATP synthases in membrane in situ is fixed or can vary within a certain narrow range, it will be necessary to implement the three-dimensional classification of all previously reported for different organisms subtomogram averages. Therefore, this work needs further investigation and preferably on intact mitochondria, which have not been disturbed by mechanical forces during fragmentation.

5.2. Dimer specific subunits

Multiple studies suggest that dimeric ATP synthases are stabilised by protein–protein interactions. A lot of effort was put into the identification of proteins involved in monomer–monomer interfaces within dimeric ATP synthases from various organisms. The subunit compositions of dimers from baker's yeast and green alga were extensively studied. Although the core-structures of monomeric ATP synthases in these organisms are conserved, their dimeric ATP synthases have unique dimer specific subunits that differ between species but nevertheless ensure the conservation of the angular association of monomers into dimers and oligomers.

5.2.1. Green algae

Dimeric ATP synthases of 1600 kDa from the closely related algae *Polytomella* and *Chlamydomonas* were investigated in detail. It was revealed that in both enzymes the main components of complex V are subunits α, ß, γ, δ, a, c and OSCP. The peripheral stalk subunits A6L, b, d, f, F6 and dimer specific subunits e and g, which are typical for the bovine enzyme, are absent in algal enzymes. Instead, they contain nine

specific subunits in the range of 9 to 66 kDa named ASA1 to ASA9 (for ATP Synthase Associated) [68,69], which seem to be shared by other members of Chlorophyceae [70]. The topology of these subunits was extensively studied by cross-linking and partial dissociation of the *Polytomella* supercomplex either in membranes [71] or in isolation [67]. Based on these approaches two different models were proposed [67,71] for the localisation of subunits ASA1-9. 2D EM projections and subtomogram averages of the dimeric ATP synthase from *Polytomella* showed the presence of a large, unusually shaped peripheral stalk [8,19], which is larger than that of the yeast or bovine enzymes and likely accommodates the unrelated ASA subunits. The major difference between two models is that the ASA1 subunit is proposed to constitute either the bulky peripheral stalk [71] or to belong to the membrane part of ATP synthase [67]. The model suggested by van Lis et al. [71] is supported by the fact that the ASA1 subunit is water soluble and large enough (66 kDa) to fill the peripheral stalk density [71]. ASA6 and ASA9 are mainly found in the dimeric form of the enzyme and were proposed to be at the dimer–dimer interface in the membrane [67,71]. Additional experiments are required to verify the models.

5.2.2. Yeast

ATP synthase from *S. cerevisiae* comprises three additional subunits e, g and k, associated with the F_o-part. They were found in the dimeric form of the enzyme and were assigned as dimer-specific [6]. Several studies suggested the indispensable role of the dimer-specific subunits in stabilization of the monomer–monomer interface in the dimer [6,72]. Further attempts to map the subunits at the monomer–monomer interface were based on chemical cross-linking. Such studies suggested that in addition to the e, g and k subunits, a number of other subunits of the monomeric enzyme might also be involved in dimerization. It was shown that subunit 4 (b in bovine) [73], 6 (a in bovine) [4,74] of the peripheral stalk together with e and g play a major role in the ATP synthase dimerization process. The subunit 6 (F6 in bovine) of the peripheral stalk [75] and the yeast-specific subunit i form homodimers [76], which were found to be associated with ATP synthase dimers even in the absence of subunits e and g, although subunit i is not essential for the dimer formation [72]. Tomography data convincingly show the oligomeric state of the ATP synthase complex, which is the association of dimers into rows, but are far too low in resolution to reveal concrete subunit positions and interactions [20], and the dimer–dimer interface is thus less well understood. It was proposed to be stabilised via the e, g and h subunits (reviewed in [77]). In the recent cryo-ET work of fragmented mitochondria authors described the variability of angles between dimers in a row and concluded that there are no specific dimer–dimer contacts in a row [20]. Possibly, this finding should be confirmed for intact mitochondria.

Cryo-electron tomography corroborated the crucial role of subunits e, g and 4 (b) in the dimerization process. Yeast mutants without subunits e and g or the first transmembrane helix of the subunit 4 are devoid of ATP synthase dimers and lack lamellar cristae in their mitochondria. However, mitochondria appear normal in mutants missing subunit k [20]. To fully answer the question which subunits form monomer–monomer and dimer–dimer interfaces and which of them are essential for the stability of the dimers and oligomers, a high-resolution 3D structure of the dimeric ATP synthase is needed. A combination of structural and biochemical approaches will help to establish the functionally relevant subunits within the supercomplex.

5.2.3. Protozoa

Little is known about ATP synthase of protozoa. This should change in the future because the whole group of alveolates including *Tetrahymena* has an amazingly different ATP synthase subunit composition. For instance, genes encoding the subunits a and b were not detected in the genome of *Tetrahymena* [78], suggesting that ATP synthase operates in a different way in the entire clade of the Alveolata, including the malaria parasite *Plasmodium*. It also makes them an attractive potential drug target. As shown by 2D EM averaging, ATP synthase of *Tetrahymena* assembles into dimers in an unusual nearly parallel configuration and has several unique structural features (Fig. 2c, [63]). Our single particle 3D EM reconstruction of the dimeric ATP synthase from *Tetrahymena* demonstrates that ATP synthase has a typical ultrastructure with distinguishable F_o and F_1 domains that are linked by two stalks (Fig. 3). The model is relevant because it provides information about the 3D position of the monomers that cannot be deduced from the 2D averages (Fig. 2c, e). Although the 3D map does not reveal an angle between two monomers in the usual direction, it shows a displacement of the monomers by 45 Å in a direction orthogonal to the long axis through the F_o parts (Fig. 3k), as discussed below. Until now, all available structures of dimeric ATP synthases from various organisms demonstrated that the interaction between two monomeric enzymes was limited to their F_o-parts. Although there were structural hints in 2D EM averages to possible association via the peripheral stalks, which were supported by the cross-linking experiments (reviewed in [77]), they were not resolved in the 3D maps of yeast [65] and alga [19,67] due to the limited resolution. Our 3D map from *Tetrahymena* clearly shows that the monomers are linked not only via the membrane F_o-part, but are also connected via additional protein densities in the lower part of the peripheral stalks (Fig. 3f, h, j, green arrowheads). Two monomers interact with each other not in parallel, but in an antiparallel configuration in which the peripheral stalks are rotated outwards from the dimerisation axis by approximately 50º (Fig. 3a, e, i, asterisks). Remarkably, the c-rings of every monomer are not in close proximity, but are separated from each other by approximately 135 Å (Fig. 3k) and are linked via unassigned (protein) densities between them (Fig. 3f, h, l, blue arrows). Another density bridges two monomers at the intermembrane side of the dimer (Fig. 3k, dotted line). The dimeric ATP synthase in *Tetrahymena* has apparently undergone significant changes in comparison to the conventional supercomplexes from yeast and bovine. These changes have resulted in an unusual structure that requires additional protein densities to stabilise the unique construction of the protozoan enzyme. Proteomic analysis identified at least 13 novel proteins that constitute subunits apparently limited to the ciliate lineage [63]. A mitochondrially encoded protein, Ymf66 with eight predicted transmembrane domains could be a substitute for the subunit a of the F_o sector [63]. Other subunits might also constitute unknown protein domains of the dimeric ATP synthase.

5.3. Functions of the dimeric ATP synthase

Oligomerisation of ATP synthases in cristae must have a special reason. The angular association of ATP synthases in membranes points to the possible role of complex V in a local bending of the cristae membrane. Indeed, tomography studies of cristae membranes from various organisms revealed ATP synthases in highly curved areas of cristae [18–20]. It is likely that the shape of the curved dimers causes the membrane curvature, rather than that a curved membrane induces the kink in the ATP synthase dimers. The observations that disrupted mitochondria retain the bent membranes [18–20] and that isolated dimers keep their shape [8,9,62] strongly points to their active role in shaping the cristae. Additionally, yeast mutants devoid of the dimer-specific e and g subunits and lacking ATP synthase dimers have an abnormal inner membrane ultrastructure. The mitochondrial membranes of these mutant strains exhibit unusual onion- [72,79] or balloon-shaped morphology [21]. This strongly indicates that the dimerization of ATP synthases is essential for cristae formation. One of the main consequences of the membrane bending is creating a large surface area to accommodate more OXPHOS complexes. Furthermore, it has been proposed that in lamella-type mitochondria protons are directed along flat membrane surfaces from the respiratory complexes towards ATP synthases at the ridges of cristae, thus optimizing local proton concentration for ATP synthesis [21].

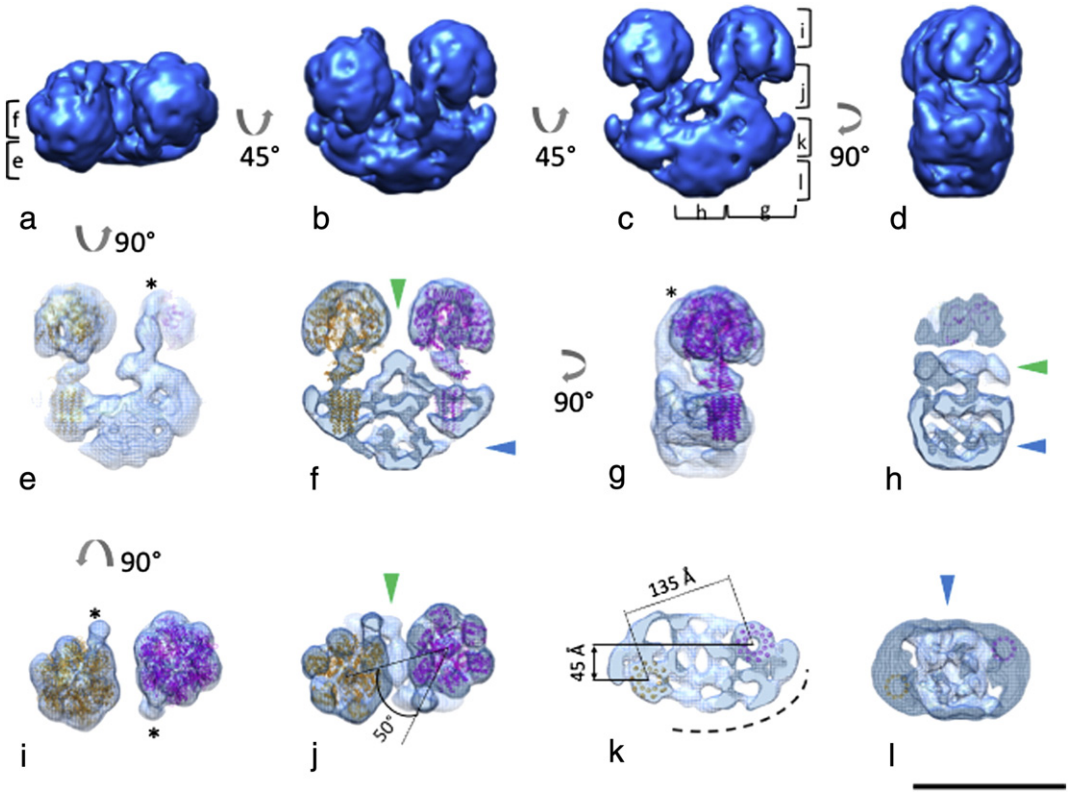

Fig. 3. Three-dimensional density map of ATP synthase dimer from *Tetrahymena thermophila*. The model was reconstructed from ~6,000 particles selected from a data set of ~50,000 particles [63] on the basis of equal representation of different views. An initial 3D model was obtained using the angular reconstitution technique in IMAGIC [83,84]. Although no symmetry was used for initial reconstruction, C2 symmetry was imposed prior the first refinement round to improve signal to noise ratio. After the first round of refinement the symmetry was relaxed to C1 (no symmetry). Further refinement of the model was done by a combination of projection matching in SPIDER [85] and angular reconstitution in IMAGIC [84]. The atomic model of ATP synthase rotor subunits with the αβ trimer (PDB ID: 2XOK, [81]) was docked into the EM density map using automated docking procedure in Chimera [86]. Resolution of the final model was 20 Å measured at Fourier Shell Correlation 0.5 criterion. Panels a–d show surface representations of the model. Panels e–l show slices through the model with docked atomic coordinates (orange and magenta). Positions of the slices are indicated on panels a and c. An asterisk indicates the position of the peripheral stalk. Arrowheads point to the densities, which bridge two ATP synthase monomers. Green arrowhead points at the junction on the level of the water-soluble parts of the peripheral stalks in F_1 subunits. Blue arrowhead indicates the large density, which is joined with F_o subunits on the intermembrane side. Dashed line arc indicates extensive peripheral densities bridging two monomers on the level of the c-subunit rings in the membrane. The scale bar is 20 nm.

There is another strong argument supporting the role of ATP synthases in the membrane curvature. ATP synthase dimers have so far only been reported for eukaryotic organisms, possibly reflecting their role in formation of mitochondrial cristae. Flat membranes in bacterial cells could have a direct link to the absence of dimerization process in prokaryotes. The subunits 4, e and g, which are essential for dimerization of ATP synthase in yeast mitochondria [6,21,73], are all encoded by nuclear DNA and might be a feature acquired during the evolution of eukaryotic organisms. It is not clear why the angular association of ATP synthases is different in *Tetrahymena* and the impact of such unusual angular arrangement on morphology and efficiency of mitochondria has to be investigated.

It is interesting to note that in ATP synthase dimers the c-subunit rings of F_o rotor parts would rotate in opposite directions with respect to the dimerization axis during proton translocation in ATP synthesis or hydrolysis. This could possibly play a role in stabilising the dimer by balancing the forces acting upon it due to the torque generated in individual ATPsynthase molecules. Additional interaction between monomers via connection of the peripheral stalks, which was observed in *Tetrahymena* and is likely present in *Polytomella* would strengthen the function of these stalks, whose primary role is to prevent the F_1-domains from rotation and which will require a greater amount of static force in dimers.

6. Future vision

In the last years, steadfast progress has been made in structural studies of the OXPHOS supercomplexes. Cryo-electron tomography experiments on mitochondrial cristae put an end to the debate about the existence of supercomplexes in mitochondria. Low-resolution structures of several supercomplexes became available, creating a framework for further functional and structural studies of the OXPHOS system. We see further progress in several directions. First of all, ongoing development of electron microscopy instrumentation and data processing in tomography and subtomogram averaging will permit more detailed studies of the respiratory chain and its physiological role in situ. Second, solving medium- and high-resolution structures of dimeric ATP synthases and respirasomes is within reach. Initial difficulties in creating the first 3D models of membrane macromolecules were overcome by the use of cryo-ET in combination with subtomogram averaging [33,80]. Finally, improvements in automated single particle image acquisition allow the collection of massive amounts of data necessary for the further refinement of structures. High-resolution studies will eventually help to identify stabilising factors for supercomplexes and particularly protein–protein interfaces in dimeric ATP synthases. Altogether, this will provide a basis for predicting mechanisms of cristae formation and modelling metabolic processes in mitochondria.

Acknowledgements

We thank Prof. A. Vaidya and Dr. N. Balabaskaran (Drexel University, USA) for providing *Tetrahymena* ATPase in an earlier stage of our research. Y.C. thanks Prof. E.V. Orlova (Birkbeck College, London) for the training in 3D single-particle EM and for the critical remarks during preparation of the manuscript. This work was supported by the Netherlands Organization of Scientific Research (NWO).

References

[1] R. Baradaran, J.M. Berrisford, G.S. Minhas, L.A. Sazanov, Crystal structure of the entire respiratory complex I, Nature 494 (2013) 443–448.
[2] R.G. Efremov, R. Baradaran, L.A. Sazanov, The architecture of respiratory complex I, Nature 465 (2010) 441–445.
[3] D. Stock, C. Gibbons, I. Arechaga, A.G. Leslie, J.E. Walker, The rotary mechanism of ATP synthase, Curr. Opin. Struct. Biol. 10 (2000) 672–679.
[4] I. Wittig, H. Schägger, Structural organization of mitochondrial ATP synthase, Biochim. Biophys. Acta 1777 (2008) 592–598.
[5] M.J. Gresser, J.A. Myers, P.D. Boyer, Catalytic site cooperativity of beef heart mitochondrial F_1 adenosine triphosphatase. Correlations of initial velocity, bound intermediate, and oxygen exchange measurements with an alternating three-site model, J. Biol. Chem. 257 (1982) 12030–12038.
[6] I. Arnold, K. Pfeiffer, W. Neupert, R.A. Stuart, H. Schägger, Yeast mitochondrial F_1F_o-ATP synthase exists as a dimer: identification of three dimer-specific subunits, EMBO J. 17 (1998) 7170–7178.
[7] H. Schägger, K. Pfeiffer, Supercomplexes in the respiratory chains of yeast and mammalian mitochondria, EMBO J. 19 (2000) 1777–1783.
[8] N.V. Dudkina, J. Heinemeyer, W. Keegstra, E.J. Boekema, H.P. Braun, Structure of dimeric ATP synthase from mitochondria: an angular association of monomers induces the strong curvature of the inner membrane, FEBS Lett. 579 (2005) 5769–5772.
[9] F. Minauro-Sanmiguel, S. Wilkens, J.J. Garcia, Structure of dimeric mitochondrial ATP synthase: novel F_o bridging features and the structural basis of mitochondrial cristae biogenesis, Proc. Natl. Acad. Sci. U. S. A. 102 (2005) 12356–12358.
[10] H. Boumans, L.A. Grivell, J.A. Berden, The respiratory chain in yeast behaves as a single functional unit, J. Biol. Chem. 273 (1998) 4872–4877.
[11] C. Bianchi, M.L. Genova, G. Parenti Castelli, G. Lenaz, The mitochondrial respiratory chain is partially organized in a supercomplex assembly: kinetic evidence using flux control analysis, J. Biol. Chem. 279 (2004) 36562–36569.
[12] R. Acin-Perez, P. Fernandez-Silva, M.L. Peleato, A. Perez-Martos, J.A. Enriquez, Respiratory active mitochondrial supercomplexes, Mol. Cell 32 (2008) 529–539.
[13] E. Lapuente-Brun, R. Moreno-Loshuertos, R. Acin-Perez, A. Latorre-Pellicer, C. Colas, E. Balsa, E. Perales-Clemente, P.M. Quiros, E. Calvo, M.A. Rodriguez-Hernandez, P. Navas, R. Cruz, A. Carracedo, C. Lopez-Otin, A. Perez-Martos, P. Fernandez-Silva, E. Fernandez-Vizarra, J.A. Enriquez, Supercomplex assembly determines electron flux in the mitochondrial electron transport chain, Science 340 (2013) 1567–1570.
[14] H. Eubel, L. Jansch, H.P. Braun, New insights into the respiratory chain of plant mitochondria. Supercomplexes and a unique composition of complex II, Plant Physiol. 133 (2003) 274–286.
[15] H. Eubel, J. Heinemeyer, H.P. Braun, Identification and characterization of respirasomes in potato mitochondria, Plant Physiol. 134 (2004) 1450–1459.
[16] J. Heinemeyer, H.P. Braun, E.J. Boekema, R. Kouril, A structural model of the cytochrome *c* reductase/oxidase supercomplex from yeast mitochondria, J. Biol. Chem. 282 (2007) 12240–12248.
[17] R.D. Allen, C.C. Schroeder, A.K. Fok, An investigation of mitochondrial inner membranes by rapid-freeze deep-etch techniques, J. Cell Biol. 108 (1989) 2233–2240.
[18] M. Strauss, G. Hofhaus, R.R. Schröder, W. Kühlbrandt, Dimer ribbons of ATP synthase shape the inner mitochondrial membrane, EMBO J. 27 (2008) 1154–1160.
[19] N.V. Dudkina, G.T. Oostergetel, D. Lewejohann, H.P. Braun, E.J. Boekema, Row-like organization of ATP synthase in intact mitochondria determined by cryo-electron tomography, Biochim. Biophys. Acta 1797 (2010) 272–277.
[20] K.M. Davies, M. Strauss, B. Daum, J.H. Kief, H.D. Osiewacz, A. Rycovska, V. Zickermann, W. Kühlbrandt, Macromolecular organization of ATP synthase and complex I in whole mitochondria, Proc. Natl. Acad. Sci. U. S. A. 108 (2011) 14121–14126.
[21] K.M. Davies, C. Anselmi, I. Wittig, J.D. Faraldo-Gomez, W. Kühlbrandt, Structure of the yeast F_1F_o-ATP synthase dimer and its role in shaping the mitochondrial cristae, Proc. Natl. Acad. Sci. U. S. A. 109 (2012) 13602–13607.
[22] S.H. Kim, R. Vlkolinsky, N. Cairns, G. Lubec, Decreased levels of complex III core protein 1 and complex V beta chain in brains from patients with Alzheimer's disease and Down syndrome, Cell. Mol. Life Sci. 57 (2000) 1810–1816.
[23] A. Bender, K.J. Krishnan, C.M. Morris, G.A. Taylor, A.K. Reeve, R.H. Perry, E. Jaros, J.S. Hersheson, J. Betts, T. Klopstock, R.W. Taylor, D.M. Turnbull, High levels of mitochondrial DNA deletions in substantia nigra neurons in aging and Parkinson disease, Nat. Genet. 38 (2006) 515–517.
[24] M. Brandon, P. Baldi, D.C. Wallace, Mitochondrial mutations in cancer, Oncogene 25 (2006) 4647–4662.
[25] M. Diehn, R.W. Cho, N.A. Lobo, T. Kalisky, M.J. Dorie, A.N. Kulp, D. Qian, J.S. Lam, L.E. Ailles, M. Wong, B. Joshua, M.J. Kaplan, I. Wapnir, F.M. Dirbas, G. Somlo, C. Garberoglio, B. Paz, J. Shen, S.K. Lau, S.R. Quake, J.M. Brown, I.L. Weissman, M.F. Clarke, Association of reactive oxygen species levels and radioresistance in cancer stem cells, Nature 458 (2009) 780–783.
[26] N.V. Dudkina, H. Eubel, W. Keegstra, E.J. Boekema, H.P. Braun, Structure of a mitochondrial supercomplex formed by respiratory-chain complexes I and III, Proc. Natl. Acad. Sci. U. S. A. 102 (2005) 3225–3229.
[27] K. Peters, N.V. Dudkina, L. Jansch, H.P. Braun, E.J. Boekema, A structural investigation of complex I and I + III_2 supercomplex from Zea mays at 11–13 Å resolution: assignment of the carbonic anhydrase domain and evidence for structural heterogeneity within complex I, Biochim. Biophys. Acta 1777 (2008) 84–93.
[28] J.B. Bultema, H.P. Braun, E.J. Boekema, R. Kouril, Megacomplex organization of the oxidative phosphorylation system by structural analysis of respiratory supercomplexes from potato, Biochim. Biophys. Acta 1787 (2009) 60–67.
[29] F. Krause, N.H. Reifschneider, D. Vocke, H. Seelert, S. Rexroth, N.A. Dencher, "Respirasome"-like supercomplexes in green leaf mitochondria of spinach, J. Biol. Chem. 279 (2004) 48369–48375.
[30] N.V. Dudkina, J. Heinemeyer, S. Sunderhaus, E.J. Boekema, H.P. Braun, Respiratory chain supercomplexes in the plant mitochondrial membrane, Trends Plant Sci. 11 (2006) 232–240.
[31] T. Tsukihara, H. Aoyama, E. Yamashita, T. Tomizaki, H. Yamaguchi, K. Shinzawa-Itoh, R. Nakashima, R. Yaono, S. Yoshikawa, The whole structure of the 13-subunit oxidized cytochrome c oxidase at 2.8 Å, Science 272 (1996) 1136–1144.
[32] E. Mileykovskaya, P.A. Penczek, J. Fang, V.K. Mallampalli, G.C. Sparagna, W. Dowhan, Arrangement of the respiratory chain complexes in *Saccharomyces cerevisiae* supercomplex III_2IV_2 revealed by single particle cryo-electron microscopy, J. Biol. Chem. 287 (2012) 23095–23103.
[33] N.V. Dudkina, M. Kudryashev, H. Stahlberg, E.J. Boekema, Interaction of complexes I, III, and IV within the bovine respirasome by single particle cryoelectron tomography, Proc. Natl. Acad. Sci. U. S. A. 108 (2011) 15196–15200.
[34] T. Althoff, D.J. Mills, J.L. Popot, W. Kühlbrandt, Arrangement of electron transport chain components in bovine mitochondrial supercomplex $I_1III_2IV_1$, EMBO J. 30 (2011) 4652–4664.
[35] I. Wittig, R. Carrozzo, F.M. Santorelli, H. Schägger, Supercomplexes and subcomplexes of mitochondrial oxidative phosphorylation, Biochim. Biophys. Acta 1757 (2006) 1066–1072.
[36] G.M. Hatch, Cardiolipin: biosynthesis, remodeling and trafficking in the heart and mammalian cells (Review), Int. J. Mol. Med. 1 (1998) 33–41.
[37] K. Pfeiffer, V. Gohil, R.A. Stuart, C. Hunte, U. Brandt, M.L. Greenberg, H. Schägger, Cardiolipin stabilizes respiratory chain supercomplexes, J. Biol. Chem. 278 (2003) 52873–52880.
[38] M. Zhang, E. Mileykovskaya, W. Dowhan, Cardiolipin is essential for organization of complexes III and IV into a supercomplex in intact yeast mitochondria, J. Biol. Chem. 280 (2005) 29403–29408.
[39] K. Shinzawa-Itoh, H. Aoyama, K. Muramoto, H. Terada, T. Kurauchi, Y. Tadehara, A. Yamasaki, T. Sugimura, S. Kurono, K. Tsujimoto, T. Mizushima, E. Yamashita, T. Tsukihara, S. Yoshikawa, Structures and physiological roles of 13 integral lipids of bovine heart cytochrome *c* oxidase, EMBO J. 26 (2007) 1713–1725.
[40] E. Sedlak, M. Panda, M.P. Dale, S.T. Weintraub, N.C. Robinson, Photolabeling of cardiolipin binding subunits within bovine heart cytochrome *c* oxidase, Biochemistry 45 (2006) 746–754.
[41] C. Lange, J.H. Nett, B.L. Trumpower, C. Hunte, Specific roles of protein-phospholipid interactions in the yeast cytochrome bc_1 complex structure, EMBO J. 20 (2001) 6591–6600.
[42] C. Arnarez, J.P. Mazat, J. Elezgaray, S.J. Marrink, X. Periole, Evidence for cardiolipin binding sites on the membrane-exposed surface of the cytochrome bc_1, J. Am. Chem. Soc. 135 (2013) 3112–3120.
[43] S. Bazan, E. Mileykovskaya, V.K. Mallampalli, P. Heacock, G.C. Sparagna, W. Dowhan, Cardiolipin-dependent reconstitution of respiratory supercomplexes from purified *Saccharomyces cerevisiae* complexes III and IV, J. Biol. Chem. 288 (2013) 401–411.
[44] K. Ikeda, S. Shiba, K. Horie-Inoue, K. Shimokata, S. Inoue, A stabilizing factor for mitochondrial respiratory supercomplex assembly regulates energy metabolism in muscle, Nat. Commun. 4 (2013) 2147.
[45] S.M. Claypool, Y. Oktay, P. Boontheung, J.A. Loo, C.M. Koehler, Cardiolipin defines the interactome of the major ADP/ATP carrier protein of the mitochondrial inner membrane, J. Cell Biol. 182 (2008) 937–950.
[46] M.K. Dienhart, R.A. Stuart, The yeast Aac2 protein exists in physical association with the cytochrome bc_1-COX supercomplex and the TIM23 machinery, Mol. Biol. Cell 19 (2008) 3934–3943.
[47] V. Strogolova, A. Furness, M. Robb-McGrath, J. Garlich, R.A. Stuart, Rcf1 and Rcf2, members of the hypoxia-induced gene 1 protein family, are critical components of the mitochondrial cytochrome bc_1-cytochrome c oxidase supercomplex, Mol. Cell. Biol. 32 (2012) 1363–1373.
[48] M. Vukotic, S. Oeljeklaus, S. Wiese, F.N. Vogtle, C. Meisinger, H.E. Meyer, A. Zieseniss, D.M. Katschinski, D.C. Jans, S. Jakobs, B. Warscheid, P. Rehling, M. Deckers, Rcf1 mediates cytochrome oxidase assembly and respirasome formation, revealing heterogeneity of the enzyme complex, Cell Metab. 15 (2012) 336–347.
[49] Y.C. Chen, E.B. Taylor, N. Dephoure, J.M. Heo, A. Tonhato, I. Papandreou, N. Nath, N.C. Denko, S.P. Gygi, J. Rutter, Identification of a protein mediating respiratory supercomplex stability, Cell Metab. 15 (2012) 348–360.
[50] S. Cogliati, C. Frezza, M.E. Soriano, T. Varanita, R. Quintana-Cabrera, M. Corrado, S. Cipolat, V. Costa, A. Casarin, L.C. Gomes, E. Perales-Clemente, L. Salviati, P. Fernandez-Silva, J.A. Enriquez, L. Scorrano, Mitochondrial cristae shape determines respiratory chain supercomplexes assembly and respiratory efficiency, Cell 155 (2013) 160–171.
[51] T. Finkel, N.J. Holbrook, Oxidants, oxidative stress and the biology of ageing, Nature 408 (2000) 239–247.
[52] M. Trouillard, B. Meunier, F. Rappaport, Questioning the functional relevance of mitochondrial supercomplexes by time-resolved analysis of the respiratory chain, Proc. Natl. Acad. Sci. U. S. A. 108 (2011) E1027–E1034.
[53] H. Kirchhoff, S. Horstmann, E. Weis, Control of the photosynthetic electron transport by PQ diffusion microdomains in thylakoids of higher plants, Biochim. Biophys. Acta 1459 (2000) 148–168.
[54] R. Acin-Perez, M.P. Bayona-Bafaluy, P. Fernandez-Silva, R. Moreno-Loshuertos, A. Perez-Martos, C. Bruno, C.T. Moraes, J.A. Enriquez, Respiratory complex III is required to maintain complex I in mammalian mitochondria, Mol. Cell 13 (2004) 805–815.
[55] F. Diaz, H. Fukui, S. Garcia, C.T. Moraes, Cytochrome *c* oxidase is required for the assembly/stability of respiratory complex I in mouse fibroblasts, Mol. Cell. Biol. 26 (2006) 4872–4881.
[56] C. Ugalde, R.J. Janssen, L.P. van den Heuvel, J.A. Smeitink, L.G. Nijtmans, Differences in assembly or stability of complex I and other mitochondrial OXPHOS complexes in inherited complex I deficiency, Hum. Mol. Genet. 13 (2004) 659–667.

[57] D. Moreno-Lastres, F. Fontanesi, I. Garcia-Consuegra, M.A. Martin, J. Arenas, A. Barrientos, C. Ugalde, Mitochondrial complex I plays an essential role in human respirasome assembly, Cell Metab. 15 (2012) 324–335.
[58] A. Stroh, O. Anderka, K. Pfeiffer, T. Yagi, M. Finel, B. Ludwig, H. Schagger, Assembly of respiratory complexes I, III, and IV into NADH oxidase supercomplex stabilizes complex I in Paracoccus denitrificans, J. Biol. Chem. 279 (2004) 5000–5007.
[59] S.J. Ramirez-Aguilar, M. Keuthe, M. Rocha, V.V. Fedyaev, K. Kramp, K.J. Gupta, A.G. Rasmusson, W.X. Schulze, J.T. van Dongen, The composition of plant mitochondrial supercomplexes changes with oxygen availability, J. Biol. Chem. 286 (2011) 43045–43053.
[60] H. Schägger, Respiratory chain supercomplexes of mitochondria and bacteria, Biochim. Biophys. Acta 1555 (2002) 154–159.
[61] L.Y. Garcia Montes de Oca, A. Chagolla-Lopez, L. Gonzalez de la Vara, T. Cabellos-Avelar, C. Gomez-Lojero, E.B. Gutierrez Cirlos, The composition of the *Bacillus subtilis* aerobic respiratory chain supercomplexes, J. Bioenerg. Biomembr. 44 (2012) 473–486.
[62] N.V. Dudkina, S. Sunderhaus, H.P. Braun, E.J. Boekema, Characterization of dimeric ATP synthase and cristae membrane ultrastructure from *Saccharomyces* and *Polytomella* mitochondria, FEBS Lett. 580 (2006) 3427–3432.
[63] P. Balabaskaran Nina, N.V. Dudkina, L.A. Kane, J.E. van Eyk, E.J. Boekema, M.W. Mather, A.B. Vaidya, Highly divergent mitochondrial ATP synthase complexes in *Tetrahymena thermophila*, PLoS Biol. 8 (2010) e1000418.
[64] D. Thomas, P. Bron, T. Weimann, A. Dautant, M.F. Giraud, P. Paumard, B. Salin, A. Cavalier, J. Velours, D. Brethes, Supramolecular organization of the yeast F_1F_o-ATP synthase, Biol. Cell. 100 (2008) 591–601.
[65] S.J. Couoh-Cardel, S. Uribe-Carvajal, S. Wilkens, J.J. Garcia-Trejo, Structure of dimeric F_1F_o-ATP synthase, J. Biol. Chem. 285 (2010) 36447–36455.
[66] N.V. Dudkina, S. Sunderhaus, E.J. Boekema, H.P. Braun, The higher level of organization of the oxidative phosphorylation system: mitochondrial supercomplexes, J. Bioenerg. Biomembr. 40 (2008) 419–424.
[67] A. Cano-Estrada, M. Vazquez-Acevedo, A. Villavicencio-Queijeiro, F. Figueroa-Martinez, H. Miranda-Astudillo, Y. Cordeiro, J.A. Mignaco, D. Foguel, P. Cardol, M. Lapaille, C. Remacle, S. Wilkens, D. Gonzalez-Halphen, Subunit–subunit interactions and overall topology of the dimeric mitochondrial ATP synthase of *Polytomella* sp, Biochim. Biophys. Acta 1797 (2010) 1439–1448.
[68] P. Cardol, D. Gonzalez-Halphen, A. Reyes-Prieto, D. Baurain, R.F. Matagne, C. Remacle, The mitochondrial oxidative phosphorylation proteome of *Chlamydomonas reinhardtii* deduced from the Genome Sequencing Project, Plant Physiol. 137 (2005) 447–459.
[69] M. Vazquez-Acevedo, P. Cardol, A. Cano-Estrada, M. Lapaille, C. Remacle, D. Gonzalez-Halphen, The mitochondrial ATP synthase of chlorophycean algae contains eight subunits of unknown origin involved in the formation of an atypical stator-stalk and in the dimerization of the complex, J. Bioenerg. Biomembr. 38 (2006) 271–282.
[70] M. Lapaille, A. Escobar-Ramirez, H. Degand, D. Baurain, E. Rodriguez-Salinas, N. Coosemans, M. Boutry, D. Gonzalez-Halphen, C. Remacle, P. Cardol, Atypical subunit composition of the chlorophycean mitochondrial F_1F_o-ATP synthase and role of Asa7 protein in stability and oligomycin resistance of the enzyme, Mol. Biol. Evol. 27 (2010) 1630–1644.
[71] R. van Lis, G. Mendoza-Hernandez, G. Groth, A. Atteia, New insights into the unique structure of the F_oF_1-ATP synthase from the chlamydomonad algae *Polytomella* sp. and *Chlamydomonas reinhardtii*, Plant Physiol. 144 (2007) 1190–1199.
[72] P. Paumard, J. Vaillier, B. Coulary, J. Schaeffer, V. Soubannier, D.M. Mueller, D. Brethes, J.P. di Rago, J. Velours, The ATP synthase is involved in generating mitochondrial cristae morphology, EMBO J. 21 (2002) 221–230.
[73] V. Soubannier, J. Vaillier, P. Paumard, B. Coulary, J. Schaeffer, J. Velours, In the absence of the first membrane-spanning segment of subunit 4(b), the yeast ATP synthase is functional but does not dimerize or oligomerize, J. Biol. Chem. 277 (2002) 10739–10745.
[74] J. Velours, C. Stines-Chaumeil, J. Habersetzer, S. Chaignepain, A. Dautant, D. Brethes, Evidence of the proximity of ATP synthase subunits 6 (a) in the inner mitochondrial membrane and in the supramolecular forms of *Saccharomyces cerevisiae* ATP synthase, J. Biol. Chem. 286 (2011) 35477–35484.
[75] R. Fronzes, T. Weimann, J. Vaillier, J. Velours, D. Brethes, The peripheral stalk participates in the yeast ATP synthase dimerization independently of e and g subunits, Biochemistry 45 (2006) 6715–6723.
[76] P. Paumard, G. Arselin, J. Vaillier, S. Chaignepain, K. Bathany, J.M. Schmitter, D. Brethes, J. Velours, Two ATP synthases can be linked through subunits i in the inner mitochondrial membrane of *Saccharomyces cerevisiae*, Biochemistry 41 (2002) 10390–10396.
[77] J. Habersetzer, W. Ziani, I. Larrieu, C. Stines-Chaumeil, M.F. Giraud, D. Brethes, A. Dautant, P. Paumard, ATP synthase oligomerization: from the enzyme models to the mitochondrial morphology, Int. J. Biochem. Cell Biol. 45 (2013) 99–105.
[78] J.A. Eisen, R.S. Coyne, M. Wu, D. Wu, M. Thiagarajan, J.R. Wortman, J.H. Badger, Q. Ren, P. Amedeo, K.M. Jones, L.J. Tallon, A.L. Delcher, S.L. Salzberg, J.C. Silva, B.J. Haas, W.H. Majoros, M. Farzad, J.M. Carlton, R.K. Smith Jr., J. Garg, R.E. Pearlman, K.M. Karrer, L. Sun, G. Manning, N.C. Elde, A.P. Turkewitz, D.J. Asai, D.E. Wilkes, Y. Wang, H. Cai, K. Collins, B.A. Stewart, S.R. Lee, K. Wilamowska, Z. Weinberg, W.L. Ruzzo, D. Wloga, J. Gaertig, J. Frankel, C.C. Tsao, M.A. Gorovsky, P.J. Keeling, R.F. Waller, N.J. Patron, J.M. Cherry, N.A. Stover, C.J. Krieger, C. del Toro, H.F. Ryder, S.C. Williamson, R.A. Barbeau, E.P. Hamilton, E. Orias, Macronuclear genome sequence of the ciliate *Tetrahymena thermophila*, a model eukaryote, PLoS Biol. 4 (2006) e286.
[79] M.F. Giraud, P. Paumard, V. Soubannier, J. Vaillier, G. Arselin, B. Salin, J. Schaeffer, D. Brethes, J.P. di Rago, J. Velours, Is there a relationship between the supramolecular organization of the mitochondrial ATP synthase and the formation of cristae? Biochim. Biophys. Acta 1555 (2002) 174–180.
[80] M. Beck, V. Lucic, F. Forster, W. Baumeister, O. Medalia, Snapshots of nuclear pore complexes in action captured by cryo-electron tomography, Nature 449 (2007) 611–615.
[81] D. Stock, A.G. Leslie, J.E. Walker, Molecular architecture of the rotary motor in ATP synthase, Science 286 (1999) 1700–1705.
[82] D.M. Rees, A.G. Leslie, J.E. Walker, The structure of the membrane extrinsic region of bovine ATP synthase, Proc. Natl. Acad. Sci. U. S. A. 106 (2009) 21597–21601.
[83] M. van Heel, Angular reconstitution: a posteriori assignment of projection directions for 3D reconstruction, Ultramicroscopy 21 (1987) 111–123.
[84] M. van Heel, G. Harauz, E.V. Orlova, R. Schmidt, M. Schatz, A new generation of the IMAGIC image processing system, J. Struct. Biol. 116 (1996) 17–24.
[85] J. Frank, M. Radermacher, P. Penczek, J. Zhu, Y. Li, M. Ladjadj, A. Leith, SPIDER and WEB: processing and visualization of images in 3D electron microscopy and related fields, J. Struct. Biol. 116 (1996) 190–199.
[86] E.F. Pettersen, T.D. Goddard, C.C. Huang, G.S. Couch, D.M. Greenblatt, E.C. Meng, T.E. Ferrin, UCSF Chimera—a visualization system for exploratory research and analysis, J. Comput. Chem. 25 (2004) 1605–1612.
[87] B. Pineau, C. Mathieu, C. Gerard-Hirne, R. De Paepe, P. Chetrit, Targeting the NAD7 subunit to mitochondria restores a functional complex I and a wild type phenotype in the *Nicotiana sylvestris* CMS II mutant lacking nad7, J. Biol. Chem. 280 (2005) 25994–26001.
[88] N.L. Taylor, J.L. Heazlewood, D.A. Day, A.H. Millar, Differential impact of environmental stresses on the pea mitochondrial proteome, Mol. Cell. Proteomics 4 (2005) 1122–1133.
[89] M. Sabar, J. Balk, C.J. Leaver, Histochemical staining and quantification of plant mitochondrial respiratory chain complexes using blue-native polyacrylamide gel electrophoresis, Plant J. 44 (2005) 893–901.
[90] R. van Lis, A. Atteia, G. Mendoza-Hernandez, D. Gonzalez-Halphen, Identification of novel mitochondrial protein components of *Chlamydomonas reinhardtii*. A proteomic approach, Plant Physiol. 132 (2003) 318–330.
[91] A. Atteia, R. van Lis, G. Mendoza-Hernandez, K. Henze, W. Martin, H. Riveros-Rosas, D. Gonzalez-Halphen, Bifunctional aldehyde/alcohol dehydrogenase (ADHE) in chlorophyte algal mitochondria, Plant Mol. Biol. 53 (2003) 175–188.
[92] E. Nubel, I. Wittig, S. Kerscher, U. Brandt, H. Schägger, Two-dimensional native electrophoretic analysis of respiratory supercomplexes from *Yarrowia lipolytica*, Proteomics 9 (2009) 2408–2418.
[93] F. Krause, C.Q. Scheckhuber, A. Werner, S. Rexroth, N.H. Reifschneider, N.A. Dencher, H.D. Osiewacz, Supramolecular organization of cytochrome c oxidase- and alternative oxidase-dependent respiratory chains in the filamentous fungus *Podospora anserina*, J. Biol. Chem. 279 (2004) 26453–26461.
[94] P. Balabaskaran Nina, J.M. Morrisey, S.M. Ganesan, H. Ke, A.M. Pershing, M.W. Mather, A.B. Vaidya, ATP synthase complex of *Plasmodium falciparum*: dimeric assembly in mitochondrial membranes and resistance to genetic disruption, J. Biol. Chem. 286 (2011) 41312–41322.
[95] H. Schägger, R. de Coo, M.F. Bauer, S. Hofmann, C. Godinot, U. Brandt, Significance of respirasomes for the assembly/stability of human respiratory chain complex I, J. Biol. Chem. 279 (2004) 36349–36353.
[96] M.F. Maas, F. Krause, N.A. Dencher, A. Sainsard-Chanet, Respiratory complexes III and IV are not essential for the assembly/stability of complex I in fungi, J. Mol. Biol. 387, 259-269.
[97] I. Marques, N.A. Dencher, A. Videira, F. Krause, Supramolecular organisation of the respiratory chain in Neurospora crassa mitochondria, Eukaryot. Cell 6, 2391-2405.
[98] D. De los Rios Castillo, M. Zarco-Zavala, S. Olvera-Sanchez, J.P. Pardo, O. Juarez, F. Martinez, G. Mendoza-Hernandez, J.J. García-Trejo, O. Flores-Herrera, A typical cristae morphology of human syncytiotrophoblast mitochondria: role for complex V, J. Biol. Chem. 286, 23911-23919.